



Embedded Classification of Local Field Potentials Recorded from Rat Barrel Cortex with Implanted Multi-Electrode Array

Conference Paper**Author(s):**

[Wang, Xiaying](#) ; Magno, Michele; Cavigelli, Lukas; Mahmud, Mufti; Cecchetto, Claudia; Vassanelli, Stefano; [Benini, Luca](#) 

Publication date:

2018

Permanent link:

<https://doi.org/10.3929/ethz-b-000291157>

Rights / license:

[In Copyright - Non-Commercial Use Permitted](#)

Originally published in:

<https://doi.org/10.1109/BIOCAS.2018.8584830>

Funding acknowledgement:

162524 - MicroLearn: Micropower Deep Learning (SNF)

Embedded Classification of Local Field Potentials Recorded from Rat Barrel Cortex with Implanted Multi-Electrode Array

Xiaying Wang^{*†}, Michele Magno^{†‡}, Lukas Cavigelli[†], Mufti Mahmud^{||§}, Claudia Cecchetto[¶], Stefano Vassanelli[§], and Luca Benini^{†‡}

[†]Dept. of Information Technology and Electrical Engineering, ETH Zürich, Switzerland [‡]DEI, University of Bologna, Italy

[§]Dept. of Biomedical Sciences, University of Padova, Italy [¶]Optical Neuroimaging Unit, OIST Graduate University, Japan

^{||}Computing and Technology, Nottingham Trent University, UK

Abstract—This paper focuses on ultra-low power embedded classification of neural activities. The machine learning (ML) algorithm has been trained using evoked local field potentials (LFPs) recorded with an implanted 16×16 multi-electrode array (MEA) from the rat barrel cortex while stimulating the whisker. Experimental results demonstrate that ML can be successfully applied to noisy single-trial LFPs. We achieved up to 95.8% test accuracy in predicting the whisker deflection. The trained ML model is successfully implemented on a low-power embedded system with an average consumption of 2.6 mW.

Index Terms—Neuroscience, Machine Learning, Brain-chip Interface, Image Processing, Bio-sensors, Implantable Sensors

I. INTRODUCTION

We continuously receive inputs from the environment, which we process and elaborate in our brain to make decisions and perform actions. Over the past decades, scientists have aimed to reconstruct sensory and other stimuli from the electrical activity of neurons. This field is referred as neural decoding. Many animal experiments are conducted for this purpose. Especially interesting are the studies on barrel cortex of rodents due to its distinctive cellular structure, organization, and functional significance [1], [2].

In order to investigate the activity of neurons, many non-invasive techniques are currently available, such as fMRI, EEG, etc. They work at low spatiotemporal resolution and have limited applications in brain-machine interfacing. Besides, the data acquired, which represent the activity of large portions of the brain, are also affected by noise coming from other parts of the body. Implantable neural probes [3], [4] provide a promising solution for acquiring localized signals from a specific population of neurons, or even from one single neuron [5]. Single metal-based electrodes were firstly used. However, with recent technological developments, high-density multi-electrode arrays (MEAs) based on CMOS process became the state-of-the-art [6]. They were introduced for large-scale high-resolution *in vitro* and, only very recently, *in vivo* applications [7]–[10].

The data acquired by these miniaturized electrode matrices are meaningless if not further processed and analyzed to extract

actionable information. In recent years, researchers have developed the powerful tool of ML and large neural networks (NNs) are successfully trained to solve challenging tasks. An example to be mentioned is the shape recognition task using simulated data of rodent whisker array [11]. However, to the best of our knowledge, no related work has been done using biological data recorded from barrel cortex. Furthermore, large NNs are computationally very expensive and require a huge amount of data sets [12]. Instead, more traditional approaches, such as support vector machines (SVMs) or naive Bayes classifiers, perform remarkably and are routinely used on smaller data sets. Their computational demands are much more affordable, allowing embedded analysis on low-power micro-controllers [13], [14].

In this paper, we present a novel approach for embedded classification of single-trial evoked LFPs recorded using a 16×16 electrode array sensor from rat barrel cortex while stimulating a whisker. The sensor is implanted *in vivo* in an anesthetized animal and 2D images are recorded over time at seven cortical depths under the scalp using three stimulation protocols. The classification method decodes the cortical activity and infers the received stimulus. Experimental results with images recorded from rat brain using this new generation of implantable sensors demonstrate that ML methods can successfully and accurately discern neural activity patterns providing useful information for the decoding. We evaluated several features and classifiers (i.e. decision tree, SVM, *k*-NN, etc.) to identify the best approach in terms of accuracy and noise robustness. Moreover, the selected features and classifier are implemented on a low-power embedded system, which will allow in the future, together with the innovative CMOS-based MEAs, real-time low-power processing of neuronal data on a miniaturized implantable system [15].

II. BACKGROUND AND SYSTEM OVERVIEW

Whiskers in rodents play a central role in collecting information about the surrounding environment and objects [1]. Therefore, a successful inference of the received stimulus is helpful for localization and object recognition. The information collected by a whisker is transmitted to the barrel cortex, which is located in the primary somatosensory cortex. It is

*Corresponding author: xiaywang@iis.ee.ethz.ch

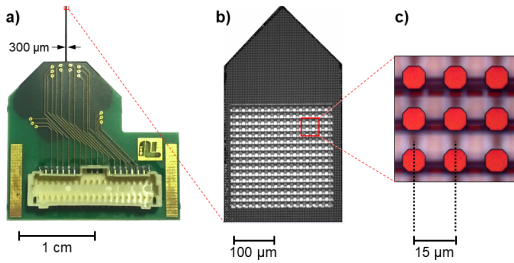


Fig. 1: Needle-PCB (a) used for data acquisition. The recording electrode array has 16×16 recording electrodes (b) spaced by $15 \mu\text{m}$ (c). Sensor provided by TU Berlin.

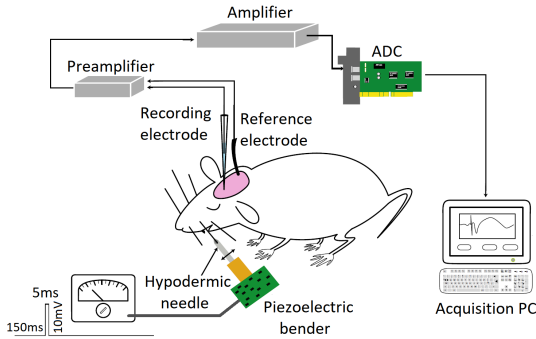


Fig. 2: Acquisition of evoked LFP responses from rat barrel cortex (S1) upon whisker deflection. Figure derived from [16].

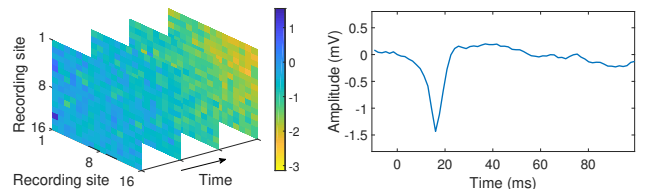
organized into a topographic map and different cortical regions are responsible for specific parts of the body. In case of whisker barrels, the topographical organization is identical to that of the mystacial pad where the major facial whiskers are located [1], [2]. The stimulation of a whisker activates the corresponding neuronal population, generating evoked LFPs, the shape and the intensity of which vary according to the type of stimulus.

The barrel cortex is organized into seven layers, considering in this paper the layers Va and Vb as separate layers. The recordings of evoked LFPs are performed *in vivo* on anesthetized rats using intra-cortical electrodes, which provide less noisy and highly localized signals. However, the intra- and inter-individual variation of bio-signals poses enormous challenges for signal decoding.

In this paper, the data are acquired using 16×16 MEAs (Fig. 1) inserted into rat barrel cortex while stimulating the principal whisker, which is identified to be the most responsive whisker for that specific barrel field, using a piezoelectric bender (Fig. 2). We evaluated and implemented ML approaches, able to accurately infer the stimulation amplitude, on a low-power embedded system.

III. DATA SET

The evoked LFPs are recorded from the barrel cortex of a single Wistar rat at the University of Padova. The recordings are performed at $15 \mu\text{m}$ resolution with a 16×16 CMOS-based sensor array [7] shown in Fig. 1. The sensory tip is inserted into the whisker barrel, while the principal whisker is stimulated by means of a piezoelectric bender. The whisker is deflected repeatedly by providing pulse stimuli of 5ms, while the signals are recorded from the topologically correspondent



(a) 2D images over time (b) Averaged signal over time
Fig. 3: Single-trial LFP images (a). One-dimensional signal (b) is obtained by averaging the images over time. The stimulus is applied at 0 ms.

receptive field in the barrel cortex.

The acquired data are two-dimensional images of 16×16 pixels over time. For each trial, 69 frames are recorded with 1.6 ms frame rate. The value of each pixel reflects the amplitude of the LFP signal in response to the whisker deflection. The matrix of electrodes is implanted into the cortex perpendicularly to the surface of the scalp. Each recording site senses the change of voltage due to the firing of neighboring neurons. Three stimulation amplitudes are applied to the piezoelectric bender, more precisely 0.5V, 1.0V and 1.4V. The respective deflection displacement, angle, linear velocity and angular velocity are listed in Table I.

The frames were recorded at seven different depths. More precisely, the bottom row of the sensory matrix is placed at $200 \mu\text{m}$ in Layer I, $350 \mu\text{m}$ in Layer II, $500 \mu\text{m}$ in Layer III, $750 \mu\text{m}$ in Layer IV, $1100 \mu\text{m}$ in Layer Va, $1500 \mu\text{m}$ in Layer Vb, and $1750 \mu\text{m}$ in Layer VI, under the scalp. For convenience, in this work the layers are numbered from 1 to 7 with layers Va, Vb and VI corresponding to 5, 6 and 7, respectively. 80 trials were recorded from each depth for each stimulation amplitude, yielding $3 \times 80 \times 7$ data points in total. Fig. 3 demonstrates an example trial with 1.4V stimulation amplitude showing some images and the averaged signal over time for Layer 7.

IV. STIMULATION CLASSIFICATION

The decoding of the neural activities is translated into stimulation classification, following the work in [17]. The goal of this paper is to design an ML model robust to noise and able to accurately infer what kind of stimulation is received by the animal based on the LFPs recorded with the MEA sensor.

1) *Pre-processing*: The data are recorded for 100 ms after the stimulation delivery. The main response peak and the following positive rebound happen within roughly the first 60 ms. With the perspective of an embedded implementation

TABLE I: Stimulation parameters using the piezoelectric bender. Linear and angular displacement ($\pm \Delta x$ and $\pm \Delta \theta$) and velocities (v and v_θ) of the principal whisker's deflection are shown for each stimulation amplitude ΔV_{pzl} .

ΔV_{pzl} (V)	$\pm \Delta x$ (μm)	$\pm \Delta \theta$ ($^\circ$)	v (mm/s)	v_θ ($^\circ/\text{ms}$)
0.5	53.0	2.0	44	1.7
1	106.0	4.2	88	3.5
1.4	150.6	6.0	125	5.0

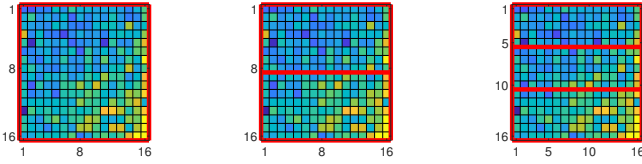


Fig. 4: Matrix subdivision for feature extraction.

on a resource-limited micro-controller, only the data of the first 60 ms, i.e. the first 38 time points, after the stimulation onset are retained. The images are then filtered spatially using a 2D Gaussian kernel (size 5×5 , $\sigma = 0.6$) and replication padding for image boundaries.

2) *Feature Extraction*: The selection of features plays a key role as it can compromise the accuracy of the classifier. The first extracted features are the mean value and the standard deviation of the images at each time point. These features provide the information of the overall trend of the evoked signal. Moreover, in order to capture the spatial information the images are divided horizontally into two and three sub-matrices (Fig. 4), as the response arises from Layer IV and spreads towards the other layers [1]. The average value and the standard deviation are computed for each sub-matrix over time. In addition, the difference between the mean values of the sub-matrices is calculated for each image to provide gradient information. Finally, 2D cross-correlation is performed between subsequent frames as shown in Fig. 5. The maximum correlation value (pointed by the red arrow) is extracted and its distance to the center of the image (x and y pixels) is used as feature. These components provide information about the direction and the intensity of the response propagation in the cortex. The template size is 10×10 , as a trade-off between the computational complexity and the accuracy of the extracted information. In fact, the bigger the template size, the higher the computational demand, while the signal-to-noise ratio (SNR) is lower in smaller templates.

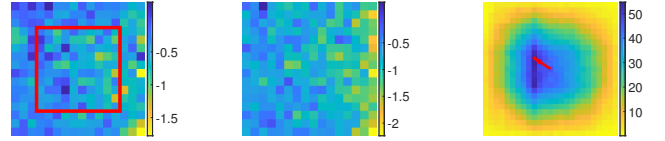
Moreover, the following features are extracted [16], [18]:

- Response Peak Amplitude (RPA): difference in voltage between Response Peak (RP) and Response Onset (RO).
- Positive Rebound (PR): absolute maximum positive value in voltage after the main response peak.
- Response Onset Latency (ROL): time delay between stimulus onset and RO.
- Response Peak Latency (RPL): time delay between stimulus onset and RP.
- time-normalized LFP (tLFP): Area Under Curve (AUC) divided by the main Response Duration (RD).

Fig. 6 shows these features on an example trial. Note that these characteristics are studied in literature on average signals of several trials. Instead, in this paper single-trial LFPs are treated. Hence, the signals in consideration are much more affected by pseudo-random physiological noise.

A. Algorithmic Procedures

The classification of stimulation amplitude is performed independently for each cortical layer, since the application requires the operator to implant the electrodes into a specific



(a) Frame at t_i (b) Frame at t_{i+1} (c) Cross-corr. map
Fig. 5: 2D cross-correlation between subsequent frames.

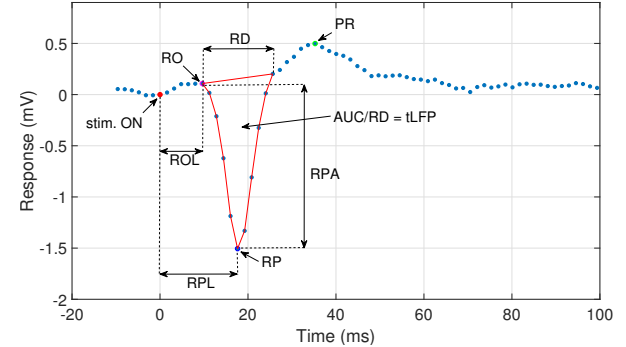


Fig. 6: Additional features extracted from the average signal.

layer, then perform the experiments. 240 data points are available for each layer. The data sets are further divided into 80% for training and cross-validation (CV) and 20% for testing.

5-fold CV is performed on the training set exploring several classifiers, i.e. decision trees, discriminant analysis, support vector machines, nearest neighbor classifiers and ensemble classifiers to identify the one which gives the best performance and determine the layer where the task is best fulfilled. Subsequently, all the possible combinations of the extracted features are evaluated to find the ones which best fulfill the task. Finally, the obtained model is tested on the testing set after tuning the hyper-parameters.

B. Embedded Implementation

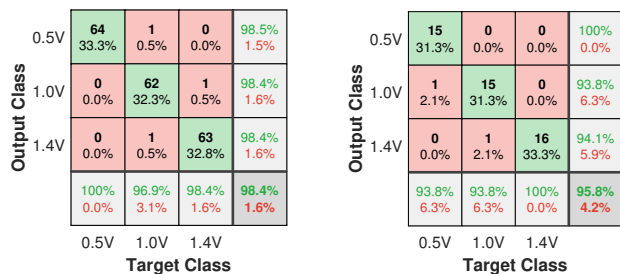
All processing steps have been implemented on an embedded low-power system to enable real-time data processing. The selected ultra-low power micro-controller is Ambiq Apollo2 with ARM Cortex-M4F processor, 256 kB RAM, 1 MB Flash memory, and a 14 bit ADC at up to 12 MS/s. The CMSIS-DSP library is exploited whenever it is possible.

The Gaussian filter is separable and has been implemented as such to reduce the computational effort. Functions such as `arm_mean_f32`, `arm_std_f32`, and `arm_sub_f32` are used to extract the statistical features and the gradients. Whereas the 2D cross-correlation is implemented exploiting the 1D correlation function of CMSIS library.

The ADC is configured to acquire $(16 \cdot 16) \cdot 38 = 9728$ samples at $(16 \cdot 16) / (1.6 \text{ ms}) = 160 \text{ kHz}$, since 38 frames are used in the designed classification model, and the frame rate is 625 Hz.

V. EXPERIMENTAL RESULTS

After the comparison among different classifications in different layers, the best performance is reached in Layer 7 with Ensemble Subspace Discriminant (ESD). Analyzing the best results for each layer, the statistical features, such as the mean and the standard deviation, and the gradients are



(a) CV confusion matrix (b) Test confusion matrix

Fig. 7: Confusion matrices. ESD with subspace dimension of 44 and 22 learning cycles on Layer 7. The features are the mean values of 2 sub-matrices, RPA, PR, RPL, and tLFP.

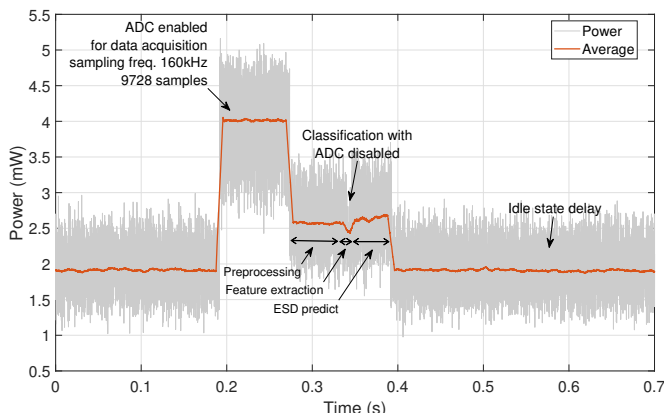


Fig. 8: Power consumption on Apollo2.

mostly included for better performance in all layers. Instead, the information provided by cross-correlation is less relevant. The subdivision of images into 3 sub-matrices resulted less useful for the task, yielding that detailed spatial information of LFP in case of stimulation classification is not crucial. In the best performance of each layer, the most frequently included feature is PR, followed by RPA, ROL, and tLFP.

Furthermore, the ESD is re-trained on Layer 7 by dividing the images into 2 sub-matrices and including the mean, RPA, PR, RPL, and tLFP. The model is re-trained by jointly tuning the two hyper-parameters. The best performance is obtained by setting subspace dimension to 44 and number of learners to 22 with CV accuracy and test accuracy reaching respectively 98.44% and 95.83%. The confusion matrices are shown in Fig. 7. The designed model is further implemented on Apollo2 with 141 kB RAM usage and 202 kB occupied Flash memory. The ADC acquires 9728 samples in 81 ms consuming 4 mW, while the model takes 119 ms for pre-processing, feature extraction, and classification, with an average consumption of 2.6 mW (Table II and Fig. 8). The execution time has the same order of magnitude as the biological time in which the sensory information reaches the cognitive areas of the animal [1].

TABLE II: Execution time on Apollo2.

Steps	Functions	Time (ms)
Data acquisition	ADC sampling	81
Preprocessing	Gaussian filtering	63
Feature Extraction	mean2, RPA, PR, RPL, tLFP	9
ESD	predict	47

VI. CONCLUSIONS

This paper proposed and evaluated a highly accurate ML approach to perform embedded stimulation classification on evoked LFPs recorded from rat barrel cortex while deflecting the principal whisker. The outcome of the paper is that ML can successfully perform automatic classification on extremely noisy data such as the single-trial LFPs and accurately infer the type of the external stimulus received by the animal, overcoming the problem of intra-individual variability of bio-signals. The system is online capable and for future improvements we plan to acquire more data from different animals using more stimulation types to train a model robust to noise due to inter-individual variability among subjects.

ACKNOWLEDGMENT

This work was funded by the Swiss National Science Foundation under grant 162524 (MicroLearn: Micropower Deep Learning).

REFERENCES

- [1] M. E Diamond *et al.*, “‘where’ and ‘what’ in the whisker sensorimotor system,” *Nature reviews. Neuroscience*, vol. 9, pp. 601–12, 08 2008.
- [2] C. C. Petersen, “The functional organization of the barrel cortex,” *Neuron*, vol. 56, no. 2, pp. 339 – 355, 2007.
- [3] K. M. Szostak *et al.*, “Microwire-cmos integration of mm-scale neural probes for chronic local field potential recording,” in *Proc. IEEE BioCAS*, Oct 2017.
- [4] V. Viswam *et al.*, “Acquisition of bioelectrical signals with small electrodes,” in *Proc. IEEE BioCAS*, Oct 2017, pp. 1–4.
- [5] G. Buzsaki *et al.*, “The origin of extracellular fields and currents: ecog, lfp and spikes,” *Nature reviews. Neuroscience*, vol. 13, 2012.
- [6] R. Thewes *et al.*, “Neural tissue and brain interfacing cmos devices #8212; an introduction to state-of-the-art, current and future challenges,” in *Proc. IEEE ISCAS*, May 2016, pp. 1826–1829.
- [7] S. Schroder *et al.*, “Cmos-compatible purely capacitive interfaces for high-density in-vivo recording from neural tissue,” in *Proc. IEEE BioCAS*, 2015.
- [8] C. Cecchetto *et al.*, “Imaging local field potentials in the rat barrel cortex,” in *Proc. ICIIBMS*, Nov 2015, pp. 296–299.
- [9] S. Vassanelli *et al.*, “On the way to large-scale and high-resolution brain-chip interfacing,” *Cognitive Computation*, vol. 4, no. 1, pp. 71–81, Mar 2012.
- [10] S. Vassanelli, “Multielectrode and multitransistor arrays for in vivo recording,” in *Nanotechnology and Neuroscience: Nano-electronic, Photonic and Mechanical Neuronal Interfacing*, M. De Vittorio *et al.*, Eds. Springer New York, 2014, pp. 239–267.
- [11] C. Zhuang *et al.*, “Toward goal-driven neural network models for the rodent whisker-trigeminal system,” *ArXiv e-prints*, Jun. 2017.
- [12] M. Mahmud *et al.*, “Applications of deep learning and reinforcement learning to biological data,” *IEEE Transactions on Neural Networks and Learning Systems*, vol. 29, no. 6, pp. 2063–2079, June 2018.
- [13] D. Sopic *et al.*, “Real-time classification technique for early detection and prevention of myocardial infarction on wearable devices,” in *Proc. IEEE BioCAS*, Oct 2017, pp. 1–4.
- [14] M. Magno *et al.*, “Energy efficient system for tactile data decoding using an ultra-low power parallel platform,” in *Proc. NGCAS*, 2017.
- [15] S. Vassanelli *et al.*, “Trends and challenges in neuroengineering: Toward intelligent neuroprostheses through brain-brain inspired systems communication,” *Frontiers in Neuroscience*, vol. 10, p. 438, 2016.
- [16] M. Mahmud *et al.*, “An automated method for characterization of evoked single-trial local field potentials recorded from rat barrel cortex under mechanical whisker stimulation,” *Cognitive Computation*, vol. 8, no. 5, pp. 935–945, Oct 2016.
- [17] X. Wang *et al.*, “Rat cortical layers classification extracting evoked local field potential images with implanted multi-electrode sensor,” in *Proc. IEEE Healthcom*, Sep 2018.
- [18] S. Temereanca *et al.*, “Local field potentials and the encoding of whisker deflections by population firing synchrony in thalamic barreloids,” *Journal of Neurophysiology*, vol. 89, no. 4, pp. 2137–2145, 2003.